

# Gradient based Adaptive Channel Estimation for Orthogonal Time Frequency Space (OTFS)

by

Divya Subhash Upalekar  
201915009

A Thesis Submitted in Partial Fulfilment of the Requirements for the Degree of

MASTER OF TECHNOLOGY  
in  
ELECTRONICS AND COMMUNICATION

with specialization in  
Wireless Communication and Embedded Systems  
to

**DHIRUBHAI AMBANI INSTITUTE OF INFORMATION AND COMMUNICATION TECHNOLOGY**

A program jointly offered with  
**C.R.RAO ADVANCED INSTITUTE OF MATHEMATICS, STATISTICS AND COMPUTER SCIENCE**



September, 2021

## Declaration

I hereby declare that

- i) the thesis comprises of my original work towards the degree of Master of Technology in Electronics and Communications at Dhirubhai Ambani Institute of Information and Communication Technology & C.R.Rao Advanced Institute of Applied Mathematics, Statistics and Computer Science, and has not been submitted elsewhere for a degree,
- ii) due acknowledgment has been made in the text to all the reference material used.

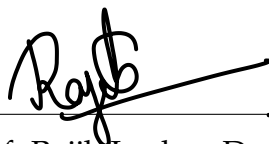


---

Divya Subhash Upalekar

## Certificate

This is to certify that the thesis work entitled Gradient based Adaptive Channel Estimation for Orthogonal Time Frequency Space (OTFS) has been carried out by Divya Subhash Upalekar for the degree of Master of Technology in Electronics and Communications at *Dhirubhai Ambani Institute of Information and Communication Technology & C.R.Rao Advanced Institute of Applied Mathematics, Statistics and Computer Science* under my/our supervision.



---

Prof. Rajib Lochan Das  
Thesis Supervisor



(Yash M. Vasavada)

---

Prof. Yash Vasavada  
Thesis Co-Supervisor

# Acknowledgments

I would like to express my sincere gratitude to my supervisor Prof. Rajib Lochan Das and co-supervisor Prof. Yash Vasavada for the continuous support, guidance and motivation. Their guidance helped me throughout in my research work and their insightful comments encouraged me to widen my research from various perspectives.

# Contents

|  |             |
|--|-------------|
| <b>Abstract</b>  | <b>vi</b>   |
| <b>List of Tables</b>  | <b>vii</b>  |
| <b>List of Figures</b>   | <b>viii</b> |
| <b>1 Introduction</b>  | <b>1</b>    |
| 1.1 Motivation . . . . .   | 1           |
| 1.2 Problem Statement . . . . .  | 2           |
| 1.3 OFDM Theory . . . . .  | 2           |
| 1.4 OFDM Drawbacks . . . . .   | 4           |
| <b>2 Orthogonal Time Frequency Space (OTFS)</b>                        | <b>7</b>    |
| 2.1 OTFS Theory . . . . .  | 7           |
| 2.1.1 Basics . . . . .   | 7           |
| 2.1.2 Principles and theorems . . . . .                                | 9           |
| 2.1.3 Key features and advantages . . . . .                            | 12          |
| 2.2 OTFS System model . . . . .  | 14          |
| 2.2.1 Block diagram . . . . .  | 14          |
| <b>3 Channel estimation</b>  | <b>19</b>   |
| 3.1 Channel representation . . . . .                                   | 19          |
| 3.2 Existing techniques . . . . .                                      | 21          |
| <b>4 Pilot based estimation</b>  | <b>23</b>   |
| <b>5 Adaptive filter theory</b>  | <b>25</b>   |
| 5.1 Background . . . . .   | 25          |
| 5.2 Some popular algorithms . . . . .                                  | 26          |
| 5.3 Least Mean Square Algorithm . . . . .                              | 26          |
| 5.4 Combination of Pilot based approach with adaptive method . . . . . | 27          |

|          |   |           |
|----------|---|-----------|
| <b>6</b> | <b>Time-Frequency domain pilot addition</b> | <b>28</b> |
| <b>7</b> | <b>Simulation results</b>                   | <b>30</b> |
| <b>8</b> | <b>Thesis Summary and Conclusion</b>        | <b>39</b> |
| <b>9</b> | <b>Future scope</b>                         | <b>40</b> |
|          | <b>References</b>                           | <b>41</b> |

# Abstract

The next generation wireless system with high mobility requirements brings the challenge to mitigate the effect of a time-varying channel. Conventional multi-carrier systems like Orthogonal frequency division multiplexing (OFDM) are designed to mitigate the multipath effects that cause Inter Symbol Interference (ISI), Since OFDM is highly sensitive to inter carrier interference (ICI), it is not well-suited for the high mobility scenarios with significant Doppler shifts and frequency dispersion. As the Doppler spread and phase noise leads to the inter carrier interference (ICI). Unlike the traditional time-frequency domain schemes, the OTFS system transmits the information symbols in the delay-Doppler domain. OTFS converts a doubly-dispersive time-frequency channel into a nearly static channel in the delay-Doppler domain by means of the Symplectic Fourier transform . In the delay-Doppler domain, the information symbols experiences constant fading, thus the OTFS system performs better than the OFDM system even in the presence of high Doppler. One of the channel estimation schemes for the OTFS system is pilot based estimation in which pilots are transmitted in the delay-Doppler domain. In this method, the delay-Doppler coordinates are estimated using the spreading of the pilot output in the time-frequency domain due to transformations. The channel coefficients estimated by these method are accurate in the absence of noise, but in the presence of noise the channel path gain value estimates were affected. Additional pilot power is required for this method to get the accurate estimate. In the proposed channel estimation algorithm, these slowly varying channel path gain values are estimated using the Gradient based adaptive algorithms. In this method the pilot based approach is combined with the adaptive methods to gain the advantages of both the methods. This method uses a single pilot symbol surrounded by some guard symbols, for the estimation of the delay-Doppler domain channel. In this method the additional pilots were inserted to support the adaptive algorithms, but it can give accurate results even in presence of noise.

**Keywords:** OTFS, Delay-Doppler domain, ZAK transform, ISFFT, SFFT, LMS.

# List of Tables

|     |       |    |
|-----|-------|----|
| 7.1 | ..... | 30 |
| 7.2 | ..... | 31 |
| 7.3 | ..... | 31 |
| 7.4 | ..... | 32 |
| 7.5 | ..... | 33 |
| 7.6 | ..... | 36 |
| 7.7 | ..... | 36 |



# List of Figures

|      |  |    |
|------|--|----|
| 1.1  | Inter Symbol Interference effect . . . . .                         | 3  |
| 1.2  | FDM vs OFDM channel . . . . .                                      | 4  |
| 1.3  | Orthogonality of Subcarriers . . . . .                             | 5  |
| 1.4  | OFDM system model . . . . .  | 5  |
| 1.5  | Effect of cyclic prefix addition . . . . .                         | 6  |
| 1.6  | Inter Carrier Interference effect . . . . .                        | 6  |
| 2.1  | Reflectors in Time-Frequency domain . . . . .                      | 8  |
| 2.2  | Reflectors in Delay-Doppler domain . . . . .                       | 8  |
| 2.3  | Delay-Doppler modulation scheme . . . . .                          | 9  |
| 2.4  | The OTFS carrier waveform transformation using ZAK transform .     | 10 |
| 2.5  | Transformation between different domains . . . . .                 | 11 |
| 2.6  | Time-Frequency and Delay-Doppler grids . . . . .                   | 11 |
| 2.7  | Symplectic Fourier transformation . . . . .                        | 12 |
| 2.8  | Key Features of OTFS . . . . .                                     | 13 |
| 2.9  | Relationship with TDM and FDM . . . . .                            | 13 |
| 2.10 | SISO-OTFS system model . . . . .                                   | 14 |
| 3.1  | $MN \times MN$ TF domain channel for $M = 8$ and $N = 8$ . . . . . | 19 |
| 3.2  | $MN \times MN$ DD domain channel for $M = 8$ and $N = 8$ . . . . . | 20 |
| 3.3  | $M \times N$ DD domain channel for $M = 32$ and $N = 32$ . . . . . | 20 |
| 3.4  | $M \times N$ TF domain channel for $M = 32$ and $N = 32$ . . . . . | 21 |
| 4.1  | $M \times N$ DD domain transmit grid . . . . .                     | 24 |
| 4.2  | Pilot grid extracted from Received signal in DD domain . . . . .   | 24 |
| 5.1  | Least Mean Square Algorithm . . . . .                              | 26 |
| 6.1  | Block type pilot rows insertion . . . . .                          | 29 |
| 6.2  | Comb and block type pilot symbols . . . . .                        | 29 |
| 7.1  | OFDM BER performance with various Doppler frequencies . . . . .    | 30 |

|      |   |    |
|------|---|----|
| 7.2  | LMS convergence plot at different step sizes . . . . .            | 31 |
| 7.3  | LMS convergence plot at different noise variances . . . . .       | 32 |
| 7.4  | OFDM BER performance with adaptive methods . . . . .              | 33 |
| 7.5  | SISO-OTFS BER performance with MMSE detector . . . . .            | 34 |
| 7.6  | Pilot output grid at pilot power 2 dB (a) and 10 dB (b) . . . . . | 35 |
| 7.7  | Estimated channel taps using adaptive algorithms . . . . .        | 35 |
| 7.8  | BER performance with block type pilot method . . . . .            | 36 |
| 7.9  | MSE performance with block type pilot method . . . . .            | 37 |
| 7.10 | BER performance with comb and block type pilot symbols . . . . .  | 37 |
| 7.11 | MSE performance with comb and block type pilot method . . . . .   | 38 |

## CHAPTER 1

# Introduction

### 1.1 Motivation

The next generation wireless networks bring substantial benefits to the users enabling significant gain in terms of productivity, speed and quality of service. The ever increasing demand of data usage makes it clear that the fourth generation networks will not be able to support these needs. Moreover applications such as high-speed trains, robotic applications are expected to overwhelm the capacity of the existing system. .

The next generation wireless systems are evolved from the drawbacks of previous generations. Thus the emerging 5G technology is evolved to support diverse usage scenarios. These systems are highly selective to the time-frequency variations and can not achieve performance compatible to the traditional multi-carrier systems. The other challenge is handling the time dispersion caused due to multipath propagation effects and the frequency dispersion caused due to the high Doppler shifts. The traditional multi-carrier systems like OFDM are affected by the Doppler shifts as it causes Inter Carrier Interference (ICI), thus leading to loss of orthogonality between the carriers.

To deal with the above mentioned problems, an approach that was taken to combat ICI and ISI in OFDM is pulse shaping. In such systems the ability to resist the time-frequency dispersion depends on the pulse localization in the time-frequency domain. However this pulse shaping approach is not adequate to deal with the doubly-dispersive channel conditions expected in future wireless systems. This pulse localization in the time-frequency domain cannot happen simultaneously due to Heisenberg's uncertainty principle.

The recently proposed two dimensional system Orthogonal Time Frequency Space(OTFS) scheme modulation has taken the motivation for mitigating the above issues. Unlike the traditional systems working in the time-frequency domain, the OTFS system is based on delay-Doppler domain representation. In the delay-

Doppler domain, the time domain pulse can be localized in delay and Doppler simultaneously.

## 1.2 Problem Statement

The OTFS system represents the the time-varying channel on any in the delay-Doppler domain. In this domain, the channel response captures the delay and Doppler spreads of the dominant reflectors. Thus estimation of the delay-Doppler domain 2D channel becomes necessary for OTFS symbol detection.

Some of the early research works which were applying the impulse based channel estimation approach require the entire OTFS frame to be transmitted for pilot transmission. This leads to reduction in spectral efficiency. To improve this further a few embedded pilot based methods have been implemented. In these methods the pilot symbols are embedded in the data grid and arranged such that there is least interference from the data symbols. This was followed by the belief propagation algorithms or threshold based methods.

Although in the delay-Doppler domain, the fast fading channel simplifies and the two-dimensional channel impulse response becomes nearly static, the delay-Doppler channel response may vary slowly with time due to high Doppler scenarios. And the existing algorithms are not well suited to handle the time-varying nature of the channel. We propose a low-complexity pilot based adaptive algorithm for estimating the 2D channel, combining the advantage of pilot assisted methods with the adaptive algorithms.

## 1.3 OFDM Theory

In the single carrier systems, the transmission occurs on the entire bandwidth in the frequency domain, thus reducing the symbol duration in the time domain. This duration becomes compatible with the delay spread defined by the difference between the arrival time of the earliest to the multipath component requiring the longest time to arrive. Thus the delay spread becomes significant as compared to the symbol duration leading to Inter Symbol Interference (ISI) shown in Figure 1.1. To deal with this issue, one way is to increase the symbol duration such that the maximum delay spread becomes negligible.

The multi-carrier systems divide the entire bandwidth into small sub-bands and dedicate each sub-band to a subcarrier. Due to this the symbol duration is increased, reducing the effectiveness of the ISI effect. But these systems require

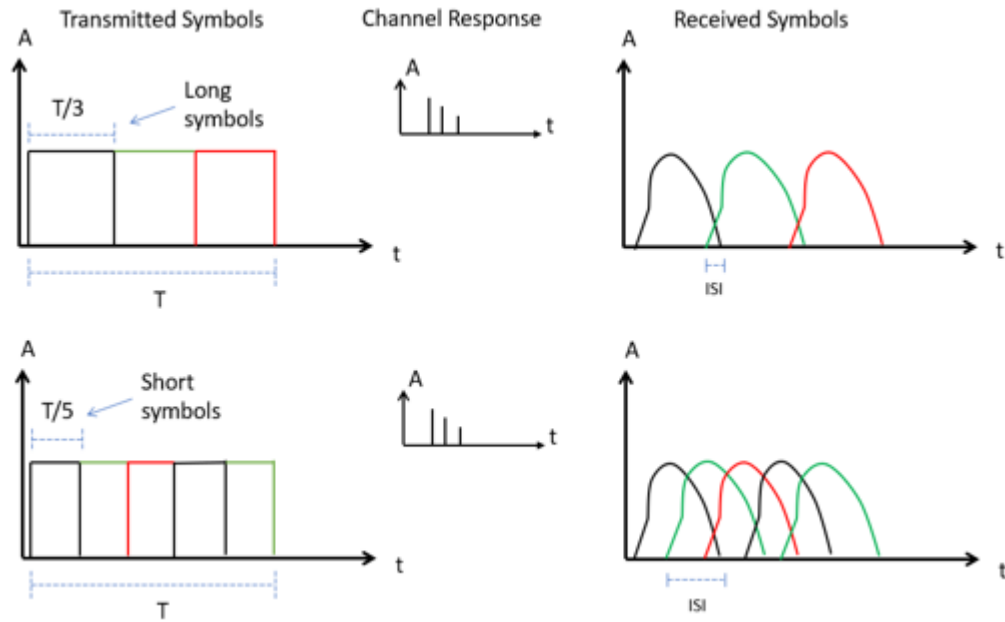


Figure 1.1: Inter Symbol Interference effect

a bank of modulators and demodulators. To implement a single modulator and demodulator block requires oscillators.

The OFDM system is a multi-carrier systems, where the subcarriers are orthogonal to each other shown in Figure 1.2. Due to orthogonality the signal spectrum corresponding to different subcarriers can be overlapped in frequency domain as shown in Figure 1.3. Hence the bandwidth efficiency can be achieved without causing ICI. In addition to orthogonality, the cyclic prefix is a key element of enabling the OFDM signal to operate reliably. The cyclic prefix is added according to the maximum delay caused by the multipath component, thus protecting the consecutive symbols from ISI.

In the OFDM system the modulation and demodulation blocks are implemented using the Inverse finite Fourier transform and finite Fourier transform respectively. Implementing a bank of  $N$  modulator or demodulator blocks is not practical as it would be computationally very complex, while the same task of modulating the  $N$ -parallel subcarriers can be done by FFT/IFFT with much less complexity. The block diagram of the OFDM system is shown in Figure 1.4. The transmitted data is the QPSK/QAM modulated symbols in the frequency domain. For transmitting this frequency domain OFDM symbol through the channel, it must be transformed to a time domain symbol using IFFT operation. At the receiver side the FFT operation is performed to convert the received signal back to the original form.

The cyclic prefix added to the time domain OFDM symbol at the transmitter

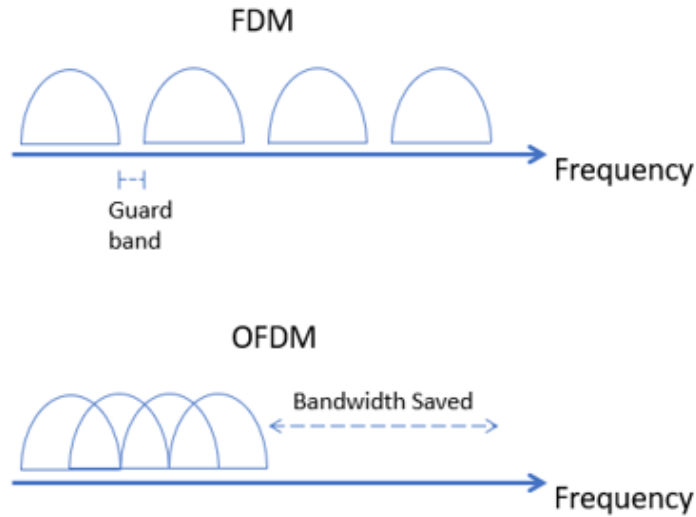


Figure 1.2: FDM vs OFDM channel

repeats the end portion of each symbol and appends it to the start of the symbol. The duration of the cyclic prefix is decided by the maximum delay spread and thus it acts like a guard between the adjacent symbols and avoids ISI. The input-output relationship in the time domain, which is represented as the linear convolution between the signal and channel, can be modeled as circular convolution due to the circular rotation caused by addition of the cyclic prefix (Figure 1.5). Due to FFT operation at the receiver this circular convolution gets transformed into multiplication thus simplifying the channel estimation and equalization.

To summarize the advantages of OFDM, it makes efficient use of the available bandwidth by overlapping the data on subcarriers in frequency domain due to orthogonality. The addition of cyclic prefix helps eliminate the ISI and converts the time-domain linear convolution to circular convolution, thus simplifying the process of frequency domain equalization. The use of the FFT block makes OFDM computationally efficient and replaces complex modulator blocks used in other multi-carrier systems.

## 1.4 OFDM Drawbacks

The OFDM system is based on certain assumptions like the time domain channel impulse response is shorter than the CP duration, there is perfect synchronization between the transmitter and receiver, the fading is slow enough that the channel can be assumed to be constant at least throughout one OFDM symbol

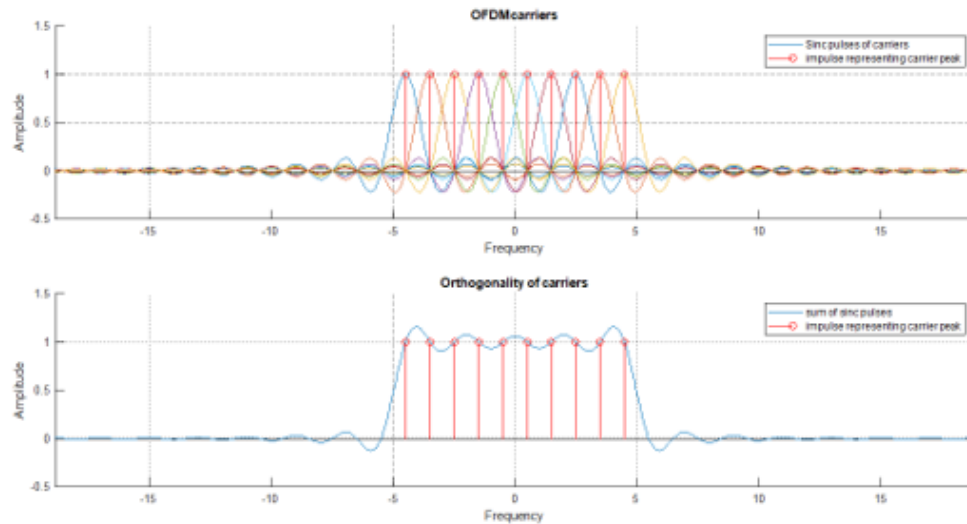


Figure 1.3: Orthogonality of Subcarriers

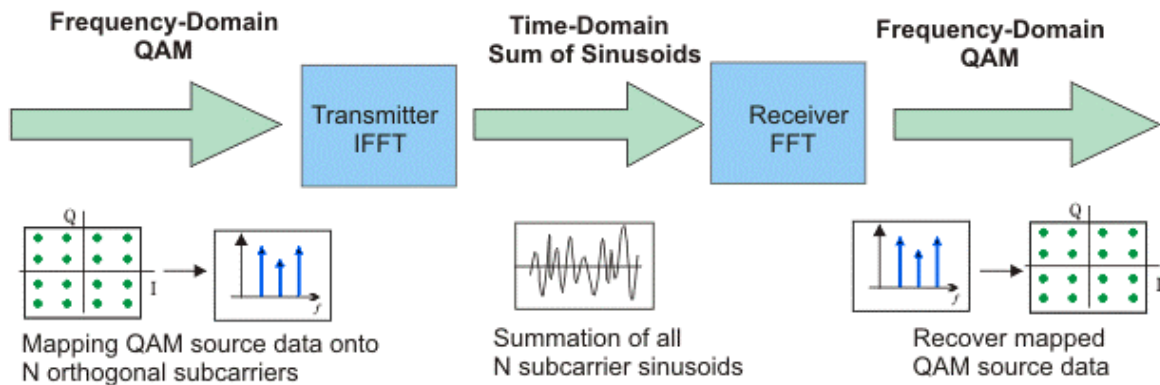


Figure 1.4: OFDM system model

length. Due to these assumptions which may not always hold, there are a few limitations that the OFDM system may face. If the cyclic prefix length is not adequate then the ISI effect will not be eliminated completely affecting the system performance. But increasing the CP length will increase the overhead thus decreasing the spectral efficiency. This is a trade-off for selecting optimum CP length.

Orthogonality is an important property that makes OFDM different and more efficient than other multi-carrier systems, but it also makes it susceptible to interference due to frequency offset. The OFDM system is more sensitive to the frequency offset, as this offset causes drift in the subcarrier spacing causing loss of orthogonality. The frequency offset often occurs when the local oscillator signal at the receiver is not synchronized with the transmitter.

The Peak to Average Power Ratio (PAPR) is the ratio of peak power to the average power of a signal. In the OFDM system due to the large number of inde-

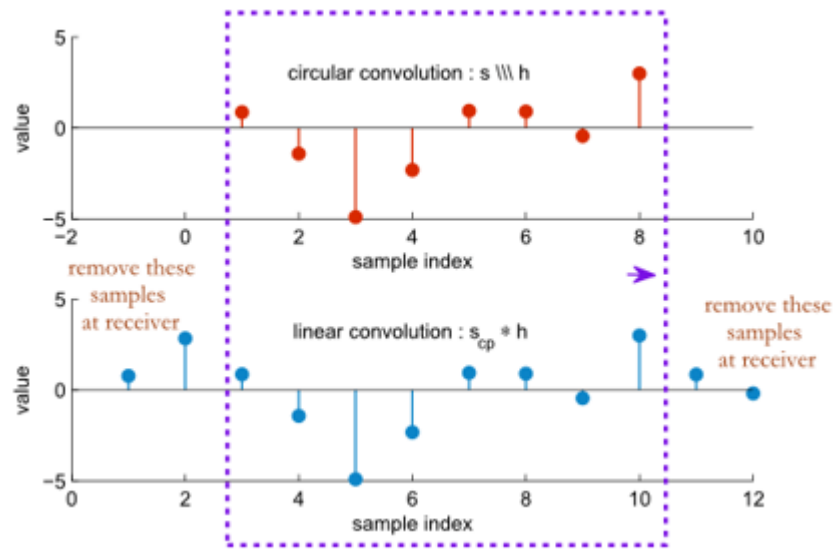


Figure 1.5: Effect of cyclic prefix addition

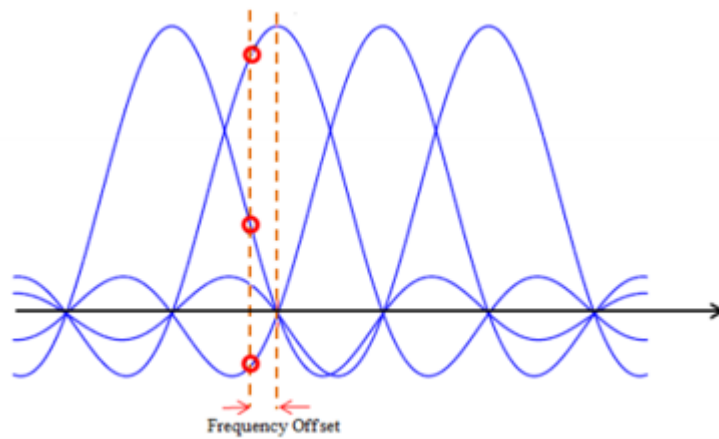


Figure 1.6: Inter Carrier Interference effect

pendent carriers the peak power can be significantly high and lead to high PAPR . Thus the signal region moves outside of the dynamic range and it crosses to the nonlinear region which results in loss of orthogonality and ICI. The effect of ICI is shown in Figure 1.6.

The OFDM is robust to the ISI in presence of time-invariant channels . However for the high mobility next generation applications, the channel is time-varying because of dispersion in both time and frequency domain. The high- speed communication causes high Doppler conditions. Due to the high Doppler shifts, the orthogonality of the subcarriers is lost and the OFDM suffers heavy performance degradation.



## CHAPTER 2

# Orthogonal Time Frequency Space (OTFS)

## 2.1 OTFS Theory

### 2.1.1 Basics

In the introduction section, we saw that the multi-carrier schemes such as OFDM eliminates the effect of inter-symbol interference (ISI)s. However they are vulnerable to the severe inter-carrier interference due to the significant Doppler spread introduced by the high-mobility scenario.

The Orthogonal Time Frequency Space (OTFS) modulation provides a potential solution for reliable communications in high-mobility scenarios. Unlike the traditional Time-Frequency (TF) domain modulation techniques like OFDM, the OTFS modulation first maps the QAM/PSK modulated symbols onto a two dimensional grid in the delay-Doppler plane. The  $M \times N$  grid has the spacing  $\Delta\tau$  along the delay period  $\tau$  and the spacing  $\Delta\nu$  along the Doppler period  $\nu$ . The delay period  $\tau_r = 1/f$  and Doppler period  $\nu_r = 1/T$  such that  $\tau \times \nu = 1$ . Thus the delay-Doppler grid is limited within unit area grid.

The OTFS waveform convolves with the wireless channel capturing the dominant multipath reflectors. In the TDM representation when a localized pulse is transmitted in time domain, at the receiver there are several echoes that correspond to the multipath delays. The phase and amplitude of these echoes changes due to Doppler shifts and the constructive or destructive interference from various reflectors sharing the same delay but differing in Doppler. Thus in the time domain, the pulses cannot be identified separately.

Similarly in the FDM representation, the FDM localized pulse gives rise to echoes corresponding to Doppler shift induced by various reflectors. Here the phase and amplitude of the echoes changes due to multipath fading effect and due to constructive or destructive interference from numerous reflectors sharing the same Doppler but differing in delay resulting in inseparability of reflectors

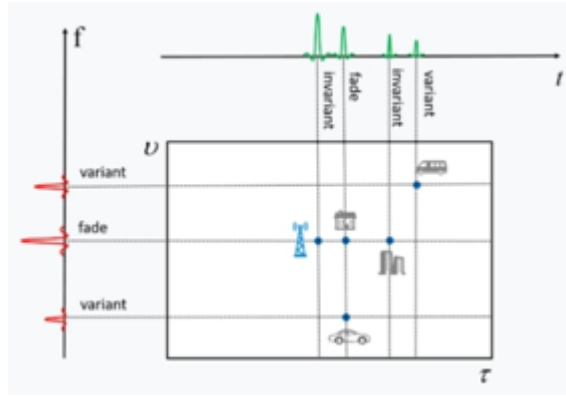


Figure 2.1: Reflectors in Time-Frequency domain

with different delay components. The TDM echoes from left to right in [[1], Figure 2.1], we can observe that the first and third echoes are due to the time invariant static reflectors, the fourth echo is due to moving reflector thus it is time varying. For the second echo there are two reflectors with same delay but different Doppler as one of the reflector is moving, so this echo is due to interference of two reflectors causing fading. Similar is the case for the second echo in frequency domain which is corresponding to fading caused due to reflectors having different delay components.

The signal represented in the delay-Doppler (DD) domain is said to be localized in both delay and Doppler domain as illustrated in [[1], Figure 2.2], which is not possible in individual time and frequency domains (Heisenberg's uncertainty principle). The reflectors can be identified separately without any fading due to this 2D delay-Doppler representation. The received echoes are confined inside the rectangular grid. Thus the transmitted pulses are separated with respect to each other and will remain orthogonal to each other.

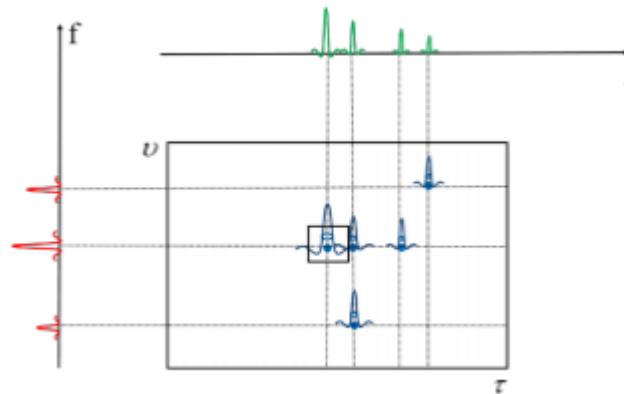


Figure 2.2: Reflectors in Delay-Doppler domain

In the OTFS system, two dimensional basis functions are used which are lo-

calized in the delay-Doppler plane. These basis functions are spread across the entire time-frequency plane when converted from delay-Doppler domain to time-frequency domain [1].

## 2.1.2 Principles and theorems

There are three ways of representing the information symbols in time, frequency and the delay-Doppler domain. The time and frequency domains can be transformed using Fourier transform. Similarly the delay-Doppler domain signal can also be converted into time-frequency domains and vice versa by the means of some transformations.

The transformation defined above is to be applied over the information symbols defined over delay-Doppler grid defined earlier. Once the grid is defined, then we position the localized pulse  $w_{m,n}$  in that delay-Doppler grid at a specific point  $(n\Delta\tau, m\Delta\nu)$ . This  $w_{m,n}$  is a two dimensional pulse shown as the combination of one-dimensional TDMA and OFDM pulses given as :

$$w_{m,n}(\tau, \nu) = w_\tau(\tau - m\Delta\tau).w_\nu(\nu - n\Delta\nu) \quad (1)$$

The first pulse is localized in the delay domain and the second one is localized in the Doppler domain as shown in Figure 2.3.

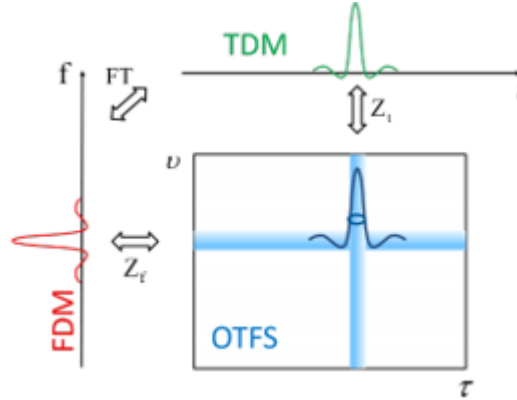


Figure 2.3: Delay-Doppler modulation scheme

To describe the pulse  $w_{m,n}$  in time domain we will compute the ZAK transform  $Z_t(w_{m,n})$  explained in detail in [2]-[3]. This time domain representation is shown as Figure 2.4. The time domain waveform is a impulse train (shown in green colour) multiplied by complex exponential signal (shown by red colour)  $e^{j2\pi m\Delta\nu t}$ . The impulses are separated by delay coordinate  $n\Delta\tau$ . The shape of the impulse train is related to the delay pulse  $w_\tau$ , and the shape of the total pulse is related

to the Fourier transform of the Doppler pulse  $w_v$ . Thus displacement along the delay axis will cause the waveform to shift along the time axis similar to TDM and the shift along the Doppler domain will cause the change in frequency by the same amount of shift like FDM. Thus OTFS can be seen as the generalization of TDM and FDM systems.

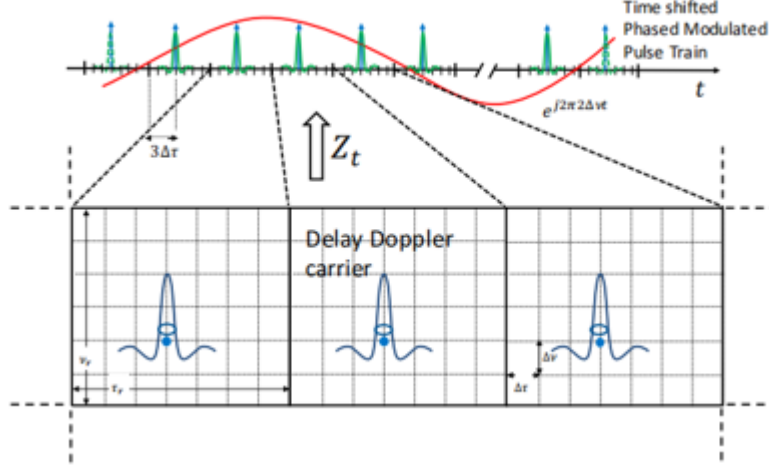


Figure 2.4: The OTFS carrier waveform transformation using ZAK transform

Another way in which the OTFS system can be modeled is by adapting the existing OFDM framework. It can be seen as a scheme that adds pre- and post-processing modules to a traditional OFDM system. This makes it more relatable with the classical multi-carrier time-frequency (TF) grid. The transformation between these grids is given by Symplectic Finite Fourier Transform (SFFT). The SFFT operation on an MN grid is equivalent to an M-dimensional FFT followed by N-dimensional IFFT along rows and columns of the grid respectively.

The motivation behind this transformation can be explained using Figure 2.5. For the transformation from delay-Doppler domain channel response  $h(\tau, v)$  to time-frequency domain channel response  $H(t, f)$ , we need to perform IFFT w.r.t. time domain to get the time-variant impulse response  $g(t, \tau)$  (time-delay domain) followed by FFT w.r.t. delay domain to get the time-frequency channel response. This operation can be performed using a single Inverse Symplectic Finite Fourier Transformation (ISFFT). And for the transformation from  $h(\tau, v)$  to  $H(t, f)$ , we need to perform FFT w.r.t. time domain to get the Doppler-variant impulse response  $B(v, f)$  (Doppler-frequency domain) followed by IFFT w.r.t. delay domain to get the delay-Doppler channel response. This operation can be performed using a single Symplectic Finite Fourier Transformation (SFFT).

This method gives another variant of OTFS, in which the OTFS system can be modeled by adapting the existing OFDM framework. It can be seen as a scheme

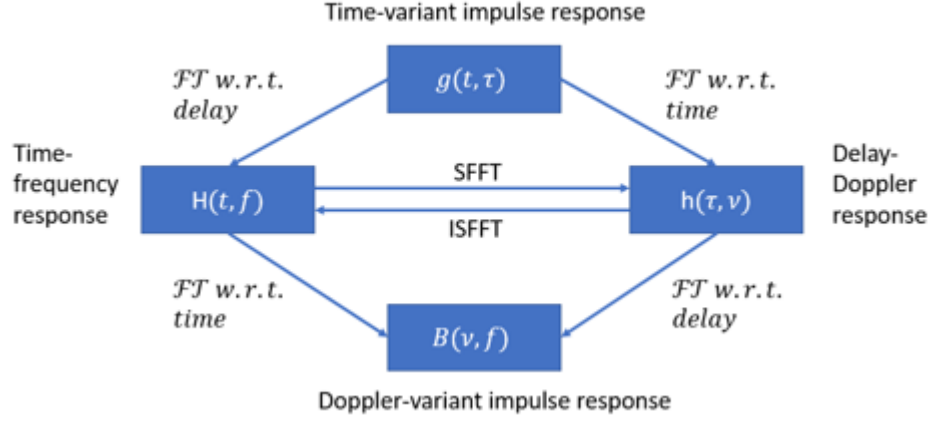


Figure 2.5: Transformation between different domains

that adds pre- and post-processing modules to a traditional OFDM system. This makes it more relatable with the classical multi-carrier time-frequency (TF) grid. The TF domain grid, with the time domain sampling interval  $T$  and the frequency domain sampling interval  $f$  is denoted as:

$$\Lambda = \{(m\Delta f, nT), m = 0, 1, \dots, M - 1, n = 0, 1, \dots, N - 1\} \quad (2)$$

While the delay-Doppler plane is discretized to an  $M$  by  $N$  grid as:

$$\Gamma = \left\{ \left( \frac{l}{M\Delta f}, \frac{k}{NT} \right), l = 0, 1, \dots, M - 1, k = 0, 1, \dots, N - 1 \right\} \quad (3)$$

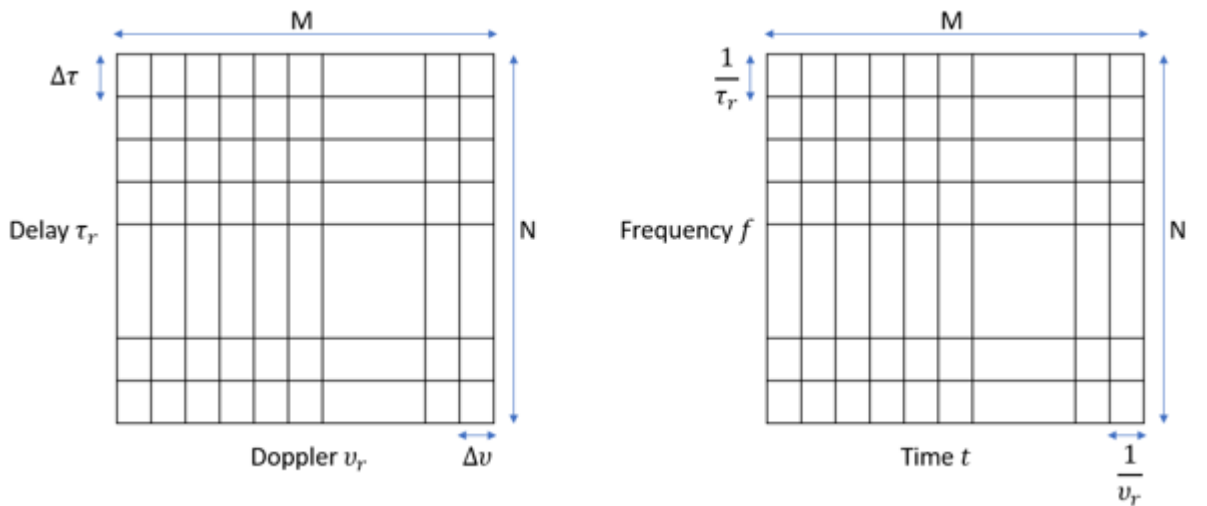


Figure 2.6: Time-Frequency and Delay-Doppler grids

Where  $\frac{1}{M\Delta f}$  and  $\frac{1}{NT}$  sampling intervals for the delay and Doppler axes re-

spectively. The time-frequency and delay-Doppler grids are shown in Figure 2.6.

The OTFS system can be viewed as the time-frequency spreading technique due to the transformation between the delay-Doppler and time-frequency domain as shown in Figure 2.7.

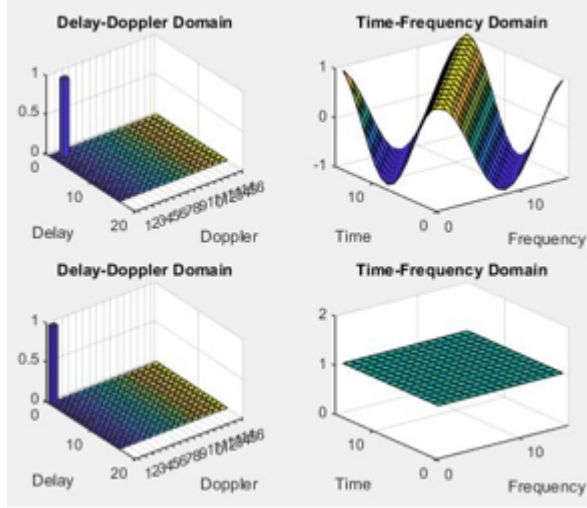


Figure 2.7: Symplectic Fourier transformation

The two dimensional (2D) orthogonal basis function that is seen above is defined as :

$$\Psi_{n,m}(m'\Delta t, n'\Delta f) = e^{j2\pi\left(\frac{mm'}{M} - \frac{nn'}{N}\right)} \quad (4)$$

As the delay and Doppler coefficients change, the slope of this 2D basis function over frequency and time axis changes as m and n respectively. This shows the analogy to the CDMA signature sequence extended to two dimensions, where these sequences are orthogonal to each other.

### 2.1.3 Key features and advantages

This section summarizes the key features and advantages of OTFS represented in Figure 2.8, which are explained in detail in the above sections.

- **Delay-Doppler domain** : The delay-Doppler representation provides a compact way to represent the signal which is localized in both delay and Doppler domain due to the property of quasi-periodicity. There is an added advantage that the channel representation in the delay-Doppler domain is sparse because of less number of multipath reflectors, which will be explained in

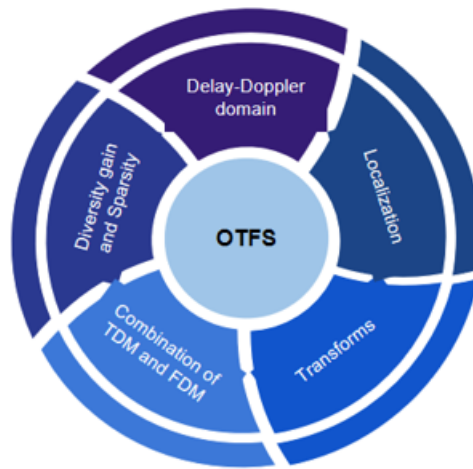


Figure 2.8: Key Features of OTFS

the next section. Due to the sparse representation the channel estimation becomes less complex.

- Transformations** : The ZAK transformation shows the relation between the TDM and FDM with OTFS system. Also the delay-Doppler grid representation equation defines hyperbola, which shows TDM and FDM as the limiting cases of OTFS as shown in Figure 2.9. The time domain representation system can be modelled as delay  $\tau_r$  tending to infinity and  $\nu_r$  tending to zero. And the frequency domain representation of the signal can be seen when  $\nu_r$  tending to infinity and  $\tau_r$  tending to zero.

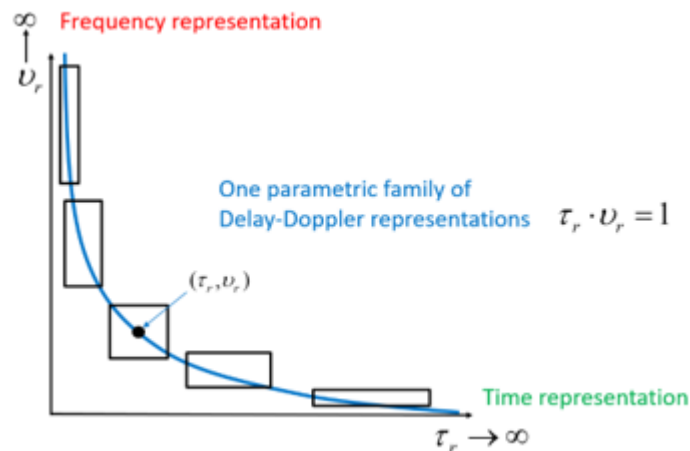


Figure 2.9: Relationship with TDM and FDM

- Diversity gain** : The Symplectic Fourier transform used for transformation from delay-Doppler domain to time-frequency domain in Figure 2.7 shows the spreading nature of the OTFS system similar to the CDMA system. Thus

the information symbol in delay-Doppler domains spans across the entire time-frequency domain resulting in diversity gain.

- **Robustness to high-Doppler channels** : The traditional multi-carrier systems suffer due to the high-Doppler induced in the channel and there is a significant degradation in performance due to the time-variant nature of the channel. On the contrary, the delay-Doppler representation of the channel converts this channel to a slow fading channel. Due to this the information symbols face near constant fading.

## 2.2 OTFS System model

### 2.2.1 Block diagram

The OTFS system follows the general block diagram as seen in [[4], Figure 2.10], where the Time-Frequency domain block is the familiar OFDM modulation scheme that is combined with the Pre and Post processing blocks to implement the OTFS modulation scheme in the delay-Doppler domain.

The QAM symbols  $x[k, l]$  arranged in the DD domain are mapped to the TF domain symbols  $X[m, n]$  through 2D Inverse Symplectic Finite Fourier Transform (ISFFT). This step is followed by the Heisenberg transform, which is a generalization of the Inverse Fast Fourier Transform (IFFT). This converts the TF domain symbols  $X[m, n]$  to the time domain signal  $s(t)$ .

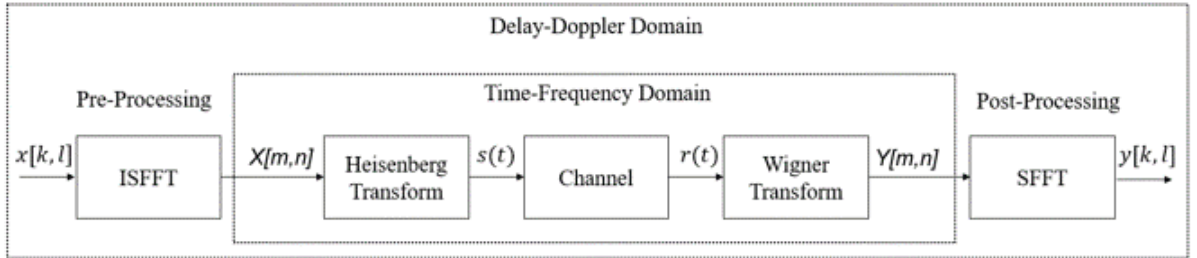


Figure 2.10: SISO-OTFS system model

The Wigner transform is applied at the receiver side on the received signal  $r(t)$  for transforming it back to a time-frequency domain signal  $Y[m, n]$ , which is a generalization of the inverse Heisenberg transform followed by the Symplectic Finite Fourier Transform (SFFT) which maps these symbols back to DD domain  $y[k, l]$ .

The OTFS system input-output relationships in different domains is expressed as follows :



1. OTFS Input-Output relation in Matrix form :

**Transmitter :**

- ISFFT:

The Symplectic Fourier Transform is a variant of the 2D Fourier transform which is used for conversion between the delay-Doppler and time-frequency channel representations. The information symbols are transmitted in a packet of duration  $NT$  in a given bandwidth  $B = M\Delta f$ , where  $\Delta f = \frac{1}{T}$ . At the transmitter side we use Inverse Symplectic Fourier Transform, given as :

$$X[m, n] = \frac{1}{MN} \sum_{k=0}^{M-1} \sum_{l=0}^{N-1} x[k, l] e^{j2\pi(\frac{nl}{N} - \frac{mk}{M})} = F_M x F_N^H \quad (5)$$

- Heisenberg transform:

This step is following the ISFFT operation known as Heisenberg transform, which maps the TF domain symbols  $X[m, n]$  to time domain signal  $s(t)$  which can be arranged in a  $M \times N$  matrix  $S$ .

$$s(t) = \sum_{m=0}^{M-1} \sum_{n=0}^{N-1} X[m, n] e^{j2\pi m\Delta f(t-nT)} \quad (6)$$

$$S = G_{tx} F_M^H X \quad (7)$$

$$S = G_{tx} F_M^H (F_M x F_N^H) = G_{tx} x F_N^H \quad (8)$$

$$s = \text{vec}(S) = (F_N^H \otimes G_{tx}) \bar{x} \quad (9)$$

where  $G_{tx}$  is the transmit window (matrix representation of  $g_{tx}$ ) and  $x$  is the DD domain  $M \times N$  grid and  $x[k, l]$  and  $\bar{x} = \text{vec}(x)$ . The equation (9) can be derived from the fact that  $\bar{x}$  is a  $MN \times 1$  vector, so to perform the same operations on the vector we should use Kronecker product.

**Channel :**

- The input-output relation in time domain is given as

$$r(t) = \int_{\tau} \int_{\nu} h(\tau, \nu) s(t - \tau) e^{j2\pi\nu(t-\tau)} d\tau d\nu + w(t) \quad (10)$$

where  $h(\tau, \nu) = \sum_{i=1}^P h_i \delta(\tau - \tau_i) \delta(\nu - \nu_i)$  is channel representation in DD domain,  $P$  is the number of propagation paths, and  $h_i, \tau_i, \nu_i$  de-

note the complex path gain, delay and Doppler shift. The delay and Doppler-shift taps for the  $i^{th}$  path are given by :  $\tau_i = \frac{l_i}{M\Delta f}, \nu_i = \frac{k_i}{NT}$  where  $l_i$  and  $k_i$  are integers and  $\Delta f$  and  $T$  are Doppler and delay resolutions.

**Receiver :**

- Wigner transform:

At the receiver side, the time domain symbols  $R$  are first converted to the TF domain samples  $Y[m, n]$  by taking the Wigner transform (OFDM demodulator) and then the SFFT on  $Y[m, n]$  to get the received symbols  $y[k, l]$  in the delay-Doppler plane.

$$Y_{tf}(f, t) = \int y(t) g_{rx}^*(t' - t) e^{-j2\pi f(t' - t)} dt' \quad (11)$$

$$Y = Y_{tf}(f, t)|_{f=m\Delta f, t=nT} = F_M G_{rx} R \quad (12)$$

- SFFT:

The Symplectic Fourier Transform for converting these TF domain symbols  $Y[m, n]$  back to DD domain symbols is given as

$$y[k, l] = \frac{1}{MN} \sum_{k=0}^{M-1} \sum_{l=0}^{N-1} Y[m, n] e^{-j2\pi(\frac{nl}{N} - \frac{mk}{M})} = F_M^H Y F_N \quad (13)$$

$$y = F_M^H (F_M G_{rx} R) F_N = G_{rx} R F_N \quad (14)$$

$$r = \text{vec}(R) \text{ and } \bar{y} = \text{vec}(y) = (F_N \otimes G_{rx}) r \quad (15)$$

where  $G_{rx}$  is the receive window.

2. OTFS Input-Output relation in Discrete form :

The received signal  $r(t)$  is sampled at the rate  $f_s = M\Delta f = \frac{M}{T}$  and a vector  $r$  of length  $MN$  is formed. The discrete form of (10) can be written as,

$$r(n) = \sum_{i=1}^P h_i e^{-j2\pi \frac{k_i(n-l_i)}{MN}} s([n-l_i]_{MN}) + w(n) \quad (16)$$

where  $[\cdot]_n$  denotes mod- $n$  operation. This equation can further be written in vector form as,

$$r = Hs + w \quad (17)$$

H is a  $MN \times MN$  matrix of the following form :

$$H = \sum_{i=1}^P h_i \Pi^{l_i} \Delta^{k_i} \quad (18)$$

where  $h_i$  is the complex channel path gain,  $\Pi$  is the permutation matrix and  $\Delta$  is the diagonal matrix. This channel is represented in Figure 3.1.

Using the equations (9), (15) and (17), the DD domain relation of transmitted and received symbols can be given as,

$$y = (F_N \otimes G_{rx})H(F_N^H \otimes G_{tx})x + (F_N \otimes G_{rx})w \quad (19)$$

$$y = H_{eff}x + \hat{w} \quad (20)$$

$H_{eff}$  is the DD domain channel shown in Figure 3.2

3. Alternate Vectorized input-output (I/O) relation : The matrix form of DD domain input-output relation which we saw in (15), can be represented alternatively as :

$$y[k, l] = \frac{1}{MN} \sum_{l'=0}^{N-1} \sum_{k'=0}^{M-1} x[k', l'] h_w \left[ \frac{(k-k')}{NT}, \frac{(l-l')}{M\Delta f} \right] + w[k, l] \quad (21)$$

where  $h_w \left[ \frac{(k-k')}{NT}, \frac{(l-l')}{M\Delta f} \right] = h_w(v, \tau) \Big|_{v=\frac{(k-k')}{NT}, \tau=\frac{(l-l')}{M\Delta f}}$  and  $h_w$  is the windowed channel response defined in [4].

4. Time-Frequency (TF) domain simplification :

In the OFDM system, the input-output relation is expressed as convolution in the time domain and multiplication in frequency domain. The OTFS system model retains this relationship. In high mobility scenarios the channel is both time and frequency dispersive due to the presence of multipath propagation and the Doppler spreads. This results in time-delay domain channel  $g(t, \tau)$ . Thus the received signal linear time variant channel can be modeled in same way as OFDM :

$$r(t) = \int g(t, \tau) s(t - \tau) d\tau + w(t) \quad (22)$$

Similarly we can express the TF domain equations as follows :

$$Y[m, n] = H[m, n] X[m, n] + ICI + ISI \quad (23)$$

The TF domain channel H and its DD domain equivalent is shown in Figure 3.4 and Figure 3.3 respectively.

## CHAPTER 3

# Channel estimation

### 3.1 Channel representation

When the information signal is transmitted over a wireless channel, it gets delayed in time (due to multipath delay spread) and its frequency content is shifted (due to Doppler shift). High mobility or high operating frequency would cause the channel to vary rapidly. The delay-Doppler representation converts the rapidly varying channel into a nearly constant or slow fading channel. Due to sparsity and compactness, the channel estimation becomes more convenient in the delay-Doppler domain than in the time-frequency domain.

In the above system model section, we have seen that the transmitted information symbols, received symbols and the channel can be represented in various formats. And depending on the representation, the channel model is also modified to suit the requirements. Thus in the matrix form, the channel in the time-frequency domain is modeled as a matrix given in (18).

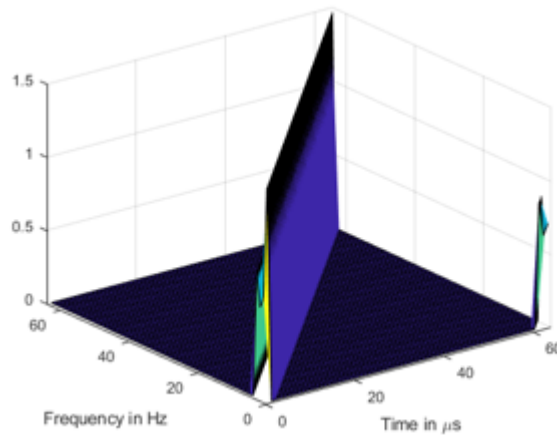


Figure 3.1:  $MN \times MN$  TF domain channel for  $M = 8$  and  $N = 8$

The delay-Doppler domain equivalent of the above channel in  $MN \times MN$  ma-

trix form  $H_{eff}$  mentioned in (20) can be written as :

$$H_{eff} = (F_N \otimes G_{rx})H(F_N^H \otimes G_{tx}) \quad (24)$$

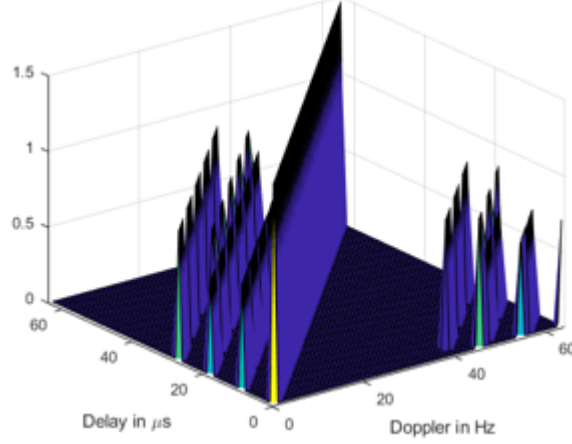


Figure 3.2:  $MN \times MN$  DD domain channel for  $M = 8$  and  $N = 8$

Both these channels are expressed as  $MN \times MN$  matrices. The windowed channel response  $h_w$  derived from the vectorized input-output relationship is the channel representation as a  $M \times N$  matrix.

$$h_w(v, \tau) = \int \int h(\tau', v') w(\tau - \tau', v - v') e^{j2\pi v \tau} d\tau' dv' \quad (25)$$

where  $w(\tau, v) = \sum_{n=0}^{N-1} \sum_{m=0}^{M-1} 1 \cdot e^{-j2\pi(vnT - \tau m \Delta f)}$

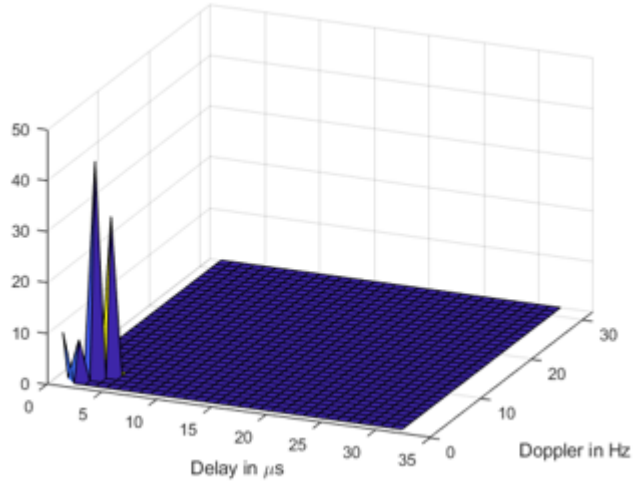


Figure 3.3:  $M \times N$  DD domain channel for  $M = 32$  and  $N = 32$

The time-frequency domain equivalent representation of this channel is given by  $H(m, n)$  (23) is shown Figure 3.4.

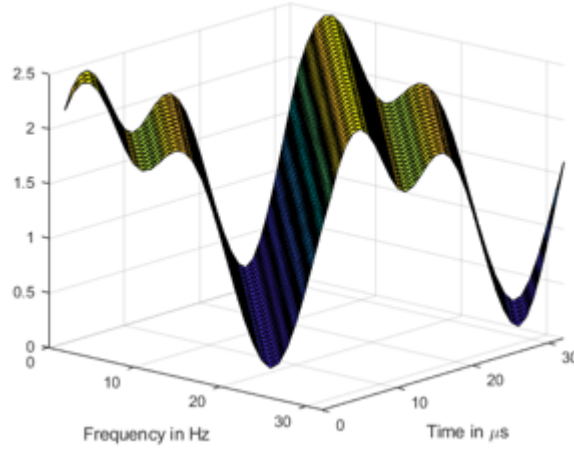


Figure 3.4:  $M \times N$  TF domain channel for  $M = 32$  and  $N = 32$

From Figure 3.3, we can see that the complex time-variant channel model is converted into a simplified form in the delay-Doppler domain. We can observe that there are four peaks in this figure, which is equal to the number of channel taps. The peaks correspond to the dominant multipath components. Thus in the delay-Doppler domain the actual geometry of the channel can be estimated.

Since there are only a few number of reflectors, the parameters to be estimated (i.e. the delay and the Doppler coefficient corresponding to the reflectors) are also fewer. Also the distance and the velocity will remain roughly the same for a larger duration of time rather than the time variant channel in time-frequency domain. This makes the channel estimation process less complex.

## 3.2 Existing techniques

In the previous chapter, we saw that the delay-Doppler domain channel estimation is less complex and also provides us the information for the complete channel response. Hence in [5]-[6], the pilot-aided channel estimation techniques were investigated. In [7], an entire OTFS frame was used for pilot transmission and the estimated channel information was used for data detection in the next frame. In this method the pilot overhead is very high. Also this method may not work well for the highly time-variant channel, as there is an assumption that the channel response will be static at least for the upcoming frame of data.

In [8] explains the time-frequency domain estimation of the channel when

compared to the [7, 9], where the channel estimation was conducted in delay–Doppler domain. The paper [6] proposed an iterative algorithm based on pseudo random pilots for channel estimation in the delay-Doppler domain. They have used the Randomized Gibbs sampling based detection algorithm, which is a complex algorithm.

In [9], the channel estimation of the OTFS system is done using the pilot-based scheme with integer Doppler shifts. But the detailed description of this scheme with the pulse shaping waveform is not given in [9]. There are several papers focusing on utilizing the sparsity of the channel and they use a compressive sensing approach for estimating the channel [10] . The compressive sensing based algorithms are complex and the pilot overhead is more.

With a suitable message passing based OTFS detection algorithm [11], the performance of OTFS is in general independent of Doppler frequencies for a given pulse shape unlike OFDM.



## CHAPTER 4

# Pilot based estimation

The traditional channel estimation methods transmit the reference symbols to estimate the channel over these symbols and then interpolate the estimated channel for the data symbols. In the OTFS system, the channel is represented in a 2D grid with respective delay-Doppler coefficients and the channel taps are less in number as compared to the whole dimension of the grid. The pilot based methods make use of the spreading property of the OTFS system i.e. the data symbol present at the position  $[m, n]$  in the delay-Doppler domain, gets spreaded across the whole time-frequency grid after the ISFFT operation [12]. Thus even with a single pilot symbol added in delay-Doppler domain, the whole time-frequency domain channel can be estimated. This eliminates the need for interpolation.

The pilot, guard and data symbol arrangement in the delay-Doppler grid for an OTFS frame transmission is as shown in Figure 4.1, where it can be seen that one pilot symbol is placed at the centre of the DD domain information symbol grid. Guard symbols are used to avoid the interference between the pilot and data symbols.

$$x[k, l] = \begin{cases} x_p, & k = \frac{M}{2}, l = \frac{N}{2} \\ 0, & \frac{M}{2} - k_v \leq k \leq \frac{M}{2} + k_v, \\ & \frac{N}{2} - l_v \leq l \leq \frac{N}{2} + l_v \\ x_d, & \text{otherwise} \end{cases} \quad (26)$$

Once this transmitted grid is converted back to the delay-Doppler domain symbols using SFFT operation, we can extract the pilot grid to estimate the channel. The pilot grid extracted from the received signal is shown in Figure 4.2, where we can observe that the single pilot symbol is spread to adjacent guard symbols due to channel impairments. The pilot symbol will undergo similar Doppler and delay shifts as experienced by the data symbols. So we can observe this pilot grid and get the delay and Doppler coefficient positions from the spreaded output.

The above shown pilot output grid is extracted in absence of noise, thus we

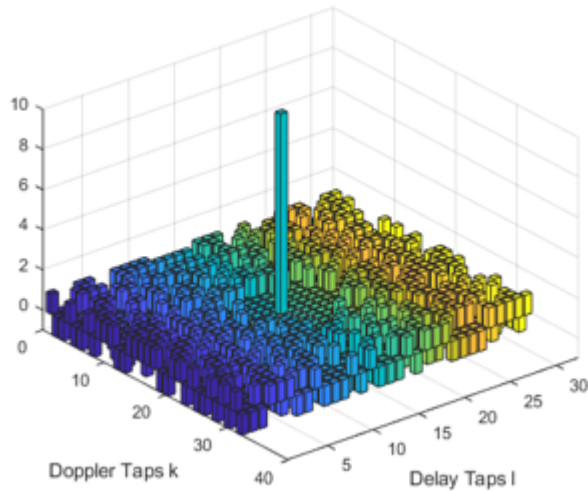


Figure 4.1:  $M \times N$  DD domain transmit grid

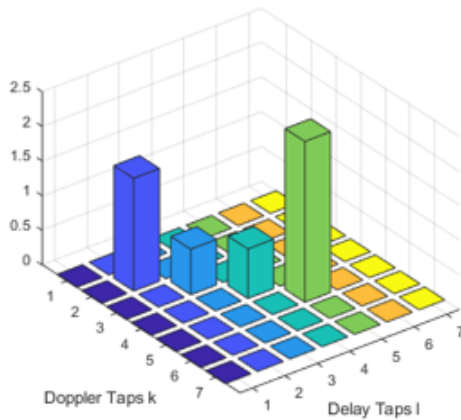


Figure 4.2: Pilot grid extracted from Received signal in DD domain

were able to retrieve the magnitude of the channel coefficients exactly from the observed peaks with the knowledge of pilot power. In the presence of noise it becomes difficult to get the channel coefficients because there might be multiple peaks in the grid and identifying the correct peaks require high pilot power.

The motivation behind going for an adaptive algorithm based approach for a high-mobility scenario was to compensate for the rapid changes in the channel. And using these algorithms, the magnitude of the channel coefficients can be determined even in the presence of noise.

## CHAPTER 5

# Adaptive filter theory

### 5.1 Background

The filter refers to a system which is used to extract the desired information from noisy data. In the communication context, because of the channel distortion and noise the data is corrupted and thus the receiver should remove this effect and estimate the original signal. In the linear filter theory consisting of Wiener or Kalman filters the algorithm tries to minimize the mean square value of error. In ref Wiener filtering based iterative Channel Estimation has been investigated for SC-FDMA. However these methods assume some prior information like mean or correlation of input or noise. So to mitigate this limitation Adaptive filters can be used.

An Adaptive filter works on recursive algorithms which modify the system parameters until error is minimized. Many adaptive algorithms can be viewed as approximations of the discrete wiener filter.

To develop the recursive algorithm for updating the system parameters (i.e channel taps in case of channel estimation problem) using the gradient based approach, we must consider the cost function. This cost function is the mean squared value of the difference between desired response and actual filter output. To get to the optimal solution the adaptive algorithm moves along the negative direction to the gradient vector direction. The adaptive algorithm developed with this concept can be expressed as :

$$W(n + 1) = W(n) + \textit{correction term} \quad (27)$$

This correction term is the product of the learning rate parameter, input vector and error signal.

## 5.2 Some popular algorithms

In the Stochastic gradient approach, the tapped- delay line model reference is used as the structural basis. From equation (27) the correction term value depends on two parameters : the correlation matrix of the tap filters and the cross correlation vector between the desired output and the input tap weights. This equation can be used to calculate the updated tap weights. This algorithm is popularly known as Least Mean Square (LMS).

$$W(n + 1) = W(n) + \mu x(n)e^*(n) \quad (28)$$

Where  $\mu$  is learning rate parameter (step size),  $x(n)$  is the input signal and  $e(n)$  is the error signal.

## 5.3 Least Mean Square Algorithm

The least-mean-square (LMS) algorithm is an adaptive filter that was first developed by Widrow and Hoff (1960). Adaptive systems can rely on a certain pre-determined criteria and can modify the system parameters to achieve optimum results. The LMS algorithm works on a simple principle of minimizing the difference between the desired response and the actual output. This simplifies the computation as this algorithm does not include any matrix operations. The block diagram is shown in Figure 5.1.

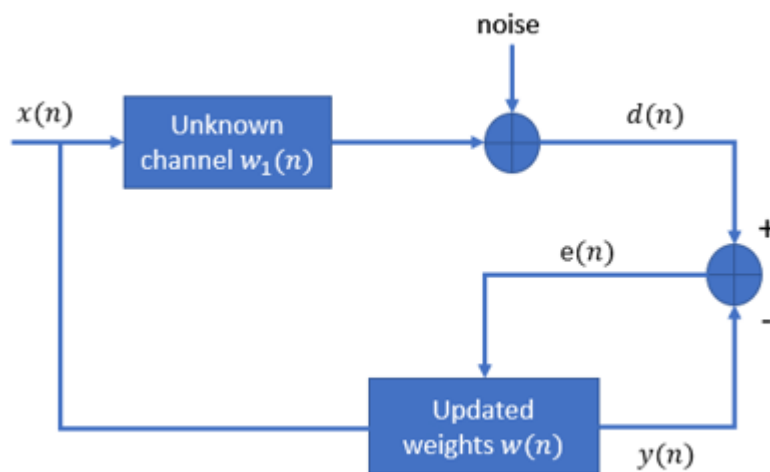


Figure 5.1: Least Mean Square Algorithm

The LMS algorithm can be summarized as follows :

Step 1 : Initialization of the channel weights to zero:  $w(0) = 0$

Step 2 : Actual output:  $y(n) = w^H x(n)$

Step 3 : Error = Expected output - Actual output:  $e(n) = d(n) - y(n)$

Step 4 : Update the channel weights:  $W(n + 1) = W(n) + \mu x(n)e^*(n)$

Where  $\mu$  is the step size.

The step size determines the convergence rate of the algorithm and the renewal amount of the channel weights. There is a trade-off between the steady state error and the convergence rate, i.e if the step size  $\mu$  is set to a high value then the algorithm can converge at a faster pace but the steady state error is proportional to the step size. This results in the decrease in accuracy. And when the step size is smaller, the steady state error value is reduced but the convergence is also achieved at comparatively lower rate.

The threshold for the convergence is step size  $\mu$  less than  $\frac{2}{\lambda_{max}}$ , where  $\lambda_{max}$  is the largest eigenvalue of the correlation matrix of the inputs [13]. When the ratio of  $\frac{\lambda_{max}}{\lambda_{min}}$  is large, then the convergence is limited by the smallest eigenvalue. To improve the convergence characteristics of the scheme we consider the Normalized LMS algorithm. The NLMS algorithm is a variant of the LMS algorithm considering step-size normalized by input signal power [14, 15, 16]. Unlike the LMS algorithm, the step-size in NLMS is time varying and given as:  $\mu = \frac{\alpha}{\beta + x^T(n)x(n)}$ , where  $\alpha$  is the adaptation constant in the range (0,2) and  $\beta \geq 0$  is the constant for normalization.

## 5.4 Combination of Pilot based approach with adaptive method

The pilot based approach is combined with the adaptive algorithms to check the performance of the OTFS channel estimation algorithm at low pilot power. The pilot based method requires high pilot power to identify the correct pilot output peaks i.e. the delay and Doppler coefficients of the channel. Also the error between the actual channel coefficients and the estimated magnitude of the channel coefficients will reduce proportionately with increase in pilot power.

The adaptive methods can be applied on the time domain data. The LMS algorithm is applied on the time domain received signal to estimate the magnitude of the channel coefficients. And the pilot based method will help us estimate the delay and Doppler coefficients. With the knowledge of these three factors we can regenerate the channel.

## CHAPTER 6

# Time-Frequency domain pilot addition

The delay-Doppler domain pilot based method had a requirement of a single pilot symbol but the pilot power required was high to correctly estimate the channel. Also the pilot needs to be surrounded by guard symbols. The adaptive algorithms were able to estimate the channel coefficients even at low pilot power but additional time domain pilots were required for channel estimation.

To achieve the channel estimation goal at low pilot power and using less number of pilots, we proposed another method where pilots can be added to time-frequency domain instead of delay-Doppler domain. The first challenge in this method was to introduce the pilot symbols in the time-frequency domain grid without disturbing the data symbols. This is because the data symbols will be spreaded across the whole time-frequency grid after ISFFT. Due to this spreading we might lose some part of the spreaded data waveform during pilot insertion. And stealing some elements from the OTFS time-frequency (TF) grid will distort all the OTFS symbols.

In the proposed algorithm a different approach is adapted rather than stealing the elements from the time-frequency grid. The delay-Doppler domain grid is designed here to be of dimension  $(N - N_p) \times M$ , where  $N_p$  is the number of pilot rows. Thus in the time-frequency domain the pilot rows will be concatenated with this grid to make the entire  $N \times M$  grid similar to the conventional block type pilot insertion method as shown in Figure 6.1. These pilot rows will be removed after channel estimation and equalization in the TF domain itself. Thus the final TF domain grid is of the dimension  $(N - N_p) \times M$  which is passed to the SFFT block.

In the above method, the rows containing pilot symbols were added to the grid. The number of pilots added will be  $N_p \times M$  which is a considerably large number. To reduce this pilot overhead, another approach was considered which is based on the combination of block and comb type pilot methods as shown in Figure 6.2 Here the number of pilot symbols gets reduced to  $N_p \times N_p$  pilot symbols

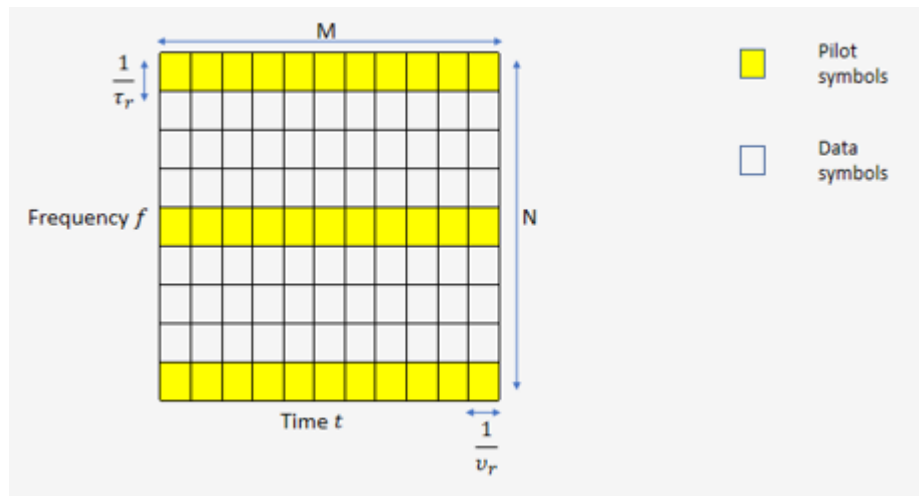


Figure 6.1: Block type pilot rows insertion

but distortion will be there due to stealing of data waveform.

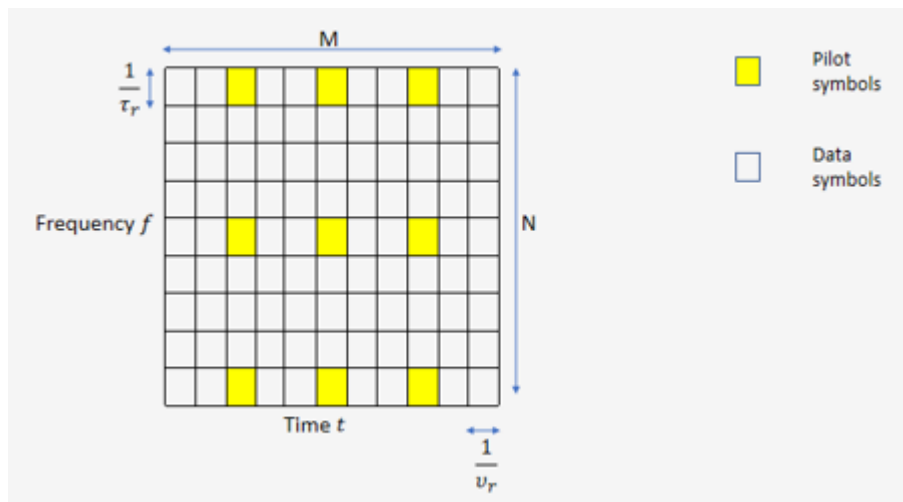


Figure 6.2: Comb and block type pilot symbols

Thus there is a trade-off between the number of pilot symbols used and the distortion caused to the data symbols which in turn will affect the BER performance.

## CHAPTER 7

# Simulation results

The MATLAB (2019a, MathWorks, Natick, MA, USA, 2019) simulator is used for the analysis. Table 7.1 shows simulation parameters for performance evaluation of OFDM systems at high Doppler frequencies. At high Doppler frequencies like 300 and 500 Hz, the BER performance is poor as compared to lower Doppler performance as observed in Figure 7.1.

| Parameters             | Value        |
|------------------------|--------------|
| FFT size ( $N_{FFT}$ ) | 100          |
| Modulation             | QPSK         |
| SNR range              | 0:25 dB      |
| Doppler spread         | 0,100,300 Hz |

Table 7.1

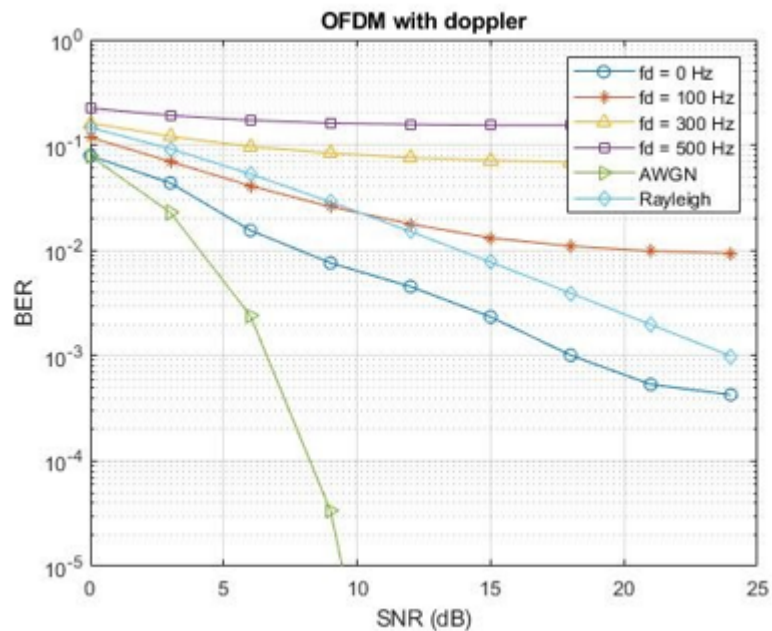


Figure 7.1: OFDM BER performance with various Doppler frequencies

The motivation behind going for an adaptive algorithm based approach for



a high-mobility scenario was to compensate for the rapid changes in the channel. The LMS algorithm was implemented for estimating the unknown channel weight  $w$  for a system  $y = wx + n$ . error between the actual channel weights and the estimated channel weights calculated and the convergence curve is plotted for 1500 iterations in the cases as shown in Figure 7.2. The Table 7.2 shows simulation parameters for LMS algorithm with varying step size.

| Parameters                    | Value            |
|-------------------------------|------------------|
| Num. of taps (L)              | 10               |
| Iterations (N)                | 1500             |
| Step size ( $\mu$ )           | [0.01,0.02,0.05] |
| Noise Variance ( $\sigma^2$ ) | 0.01             |

Table 7.2

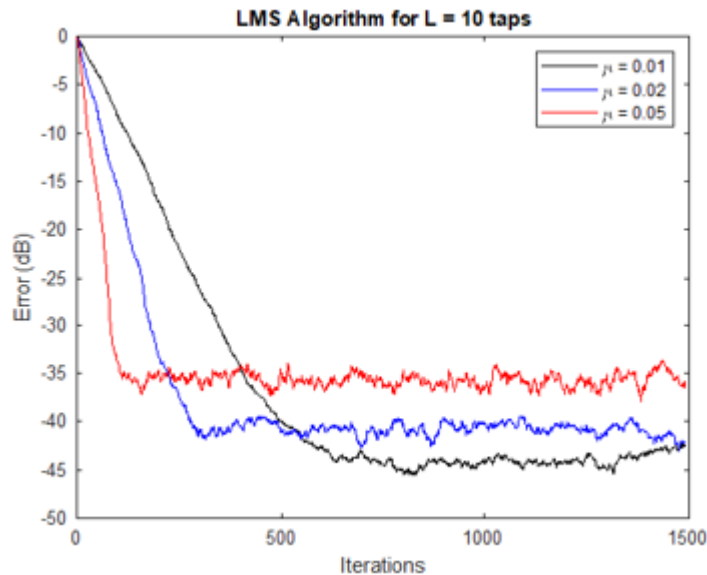


Figure 7.2: LMS convergence plot at different step sizes

| Parameters                    | Value            |
|-------------------------------|------------------|
| Num. of taps (L)              | 10               |
| Iterations (N)                | 1500             |
| Step size ( $\mu$ )           | 0.02             |
| Noise Variance ( $\sigma^2$ ) | [0.1,0.01,0.001] |

Table 7.3

With the trade-off between convergence rate and steady state error, we decided to eliminate the dependency of step size value over signal variations and apply the variants of LMS algorithms for the above system. The Table 7.3 shows

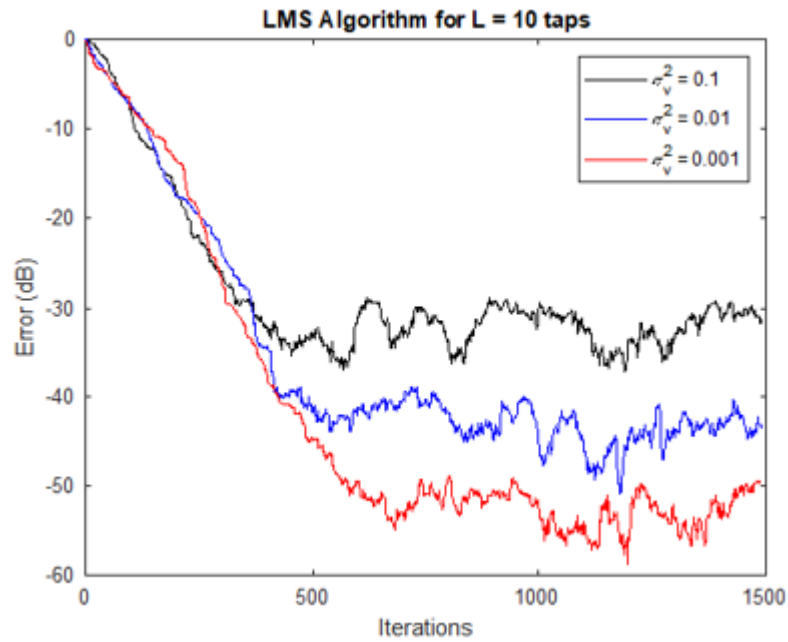


Figure 7.3: LMS convergence plot at different noise variances

simulation parameters for LMS algorithm with varying noise variance. In Figure 7.3, the convergence curve for varying noise variance is plotted. The increase in the noise variance leads to the decrease in the steady state error, but achieves a faster convergence rate.

In the initial implementation the LMS and NLMS algorithms were applied on the OFDM system with following system parameters. The BER performance of the LMS and NLMS algorithms were also compared with the traditional Least Square (LS) detector applied to the OFDM system with simulation parameters mentioned in Table 7.4. We can observe from Figure 7.4 that the NLMS algorithm's performance is comparable with the LS detector.

| Parameters                 | Value   |
|----------------------------|---------|
| Num. of subcarriers (M)    | 1024    |
| Num. f symbols (N)         | 100     |
| Length of CP ( $M_{CP}$ )  | 10      |
| Carrier frequency( $f_c$ ) | 4 GHz   |
| Subcarrier spacing (f)     | 15 KHz  |
| SNR range                  | 0:20 dB |
| Modulation scheme          | QPSK    |

Table 7.4

In this section, the demodulation performance is evaluated for the SISO-OTFS system, of which the parameters are set according to the Table 7.5. The delay-

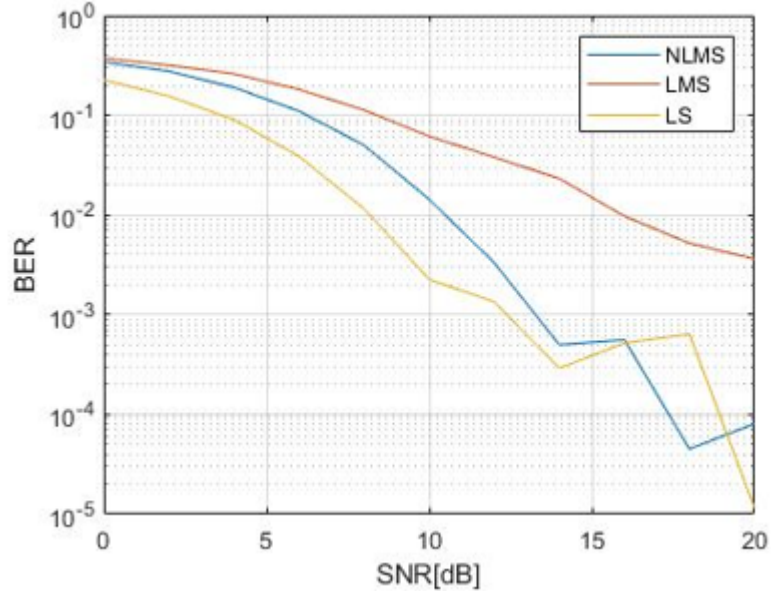


Figure 7.4: OFDM BER performance with adaptive methods

Doppler grid with  $M = 16$  and  $N = 16$  with a carrier frequency of 4 GHz and it is passed through channel has 4 multi-paths with a max delay spread of 2.08 s and max Doppler spread of 470 Hz. The BER performance of the SISO-OTFS system for the above parameters is shown in Figure 7.5.

| Parameters                  | Value   |
|-----------------------------|---------|
| Num. of subcarriers ( $M$ ) | 16      |
| Num. f symbols ( $N$ )      | 16      |
| Length of CP ( $M_{CP}$ )   | 4       |
| Carrier frequency ( $f_c$ ) | 4 GHz   |
| Subcarrier spacing ( $f$ )  | 15 KHz  |
| SNR range                   | 0:20 dB |
| Modulation scheme           | QPSK    |

Table 7.5

The LMS algorithm applied for channel estimation of OFDM was a one dimensional scheme, but the main challenge was to apply this algorithm for a 2D channel estimation of OTFS system. In some literature work on MIMO-OFDM systems two dimensional LMS algorithms were implemented [8]. They have explained the basic structure of how the LMS algorithm works for two dimensional systems.

The two dimensional LMS (TDLMS) algorithm is generally used for denoising of Image [17]-[18]. In this method for a noisy image  $x$  of dimension  $M \times M$  obtained by adding noise to the desired image  $D$  a filter window  $W$  of order  $N \times$

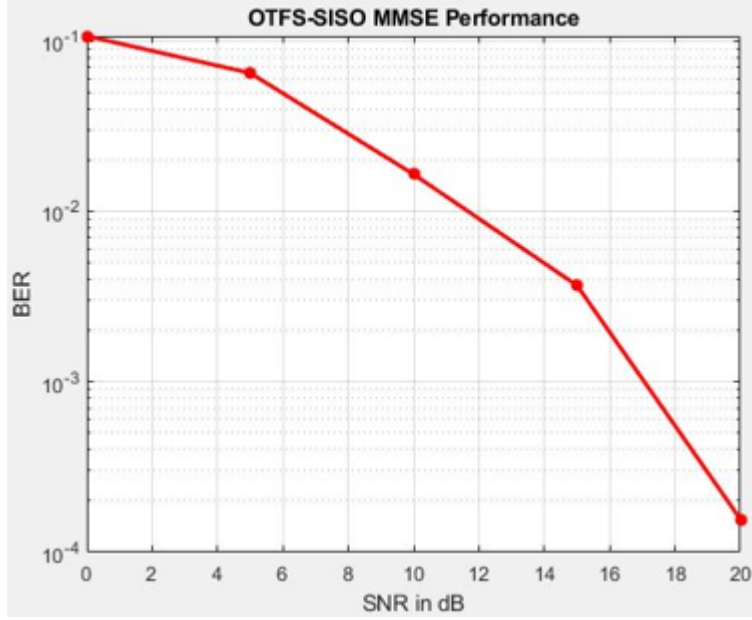


Figure 7.5: SISO-OTFS BER performance with MMSE detector

$N$  is selected. This filter window is convoluted with the  $N \times N$  portion of the image to generate the actual output which is given as,

$$y(m, n) = \sum_{l=0}^{N-1} \sum_{k=0}^{N-1} W_j(l, k) X(m-l, n-k) \quad (29)$$

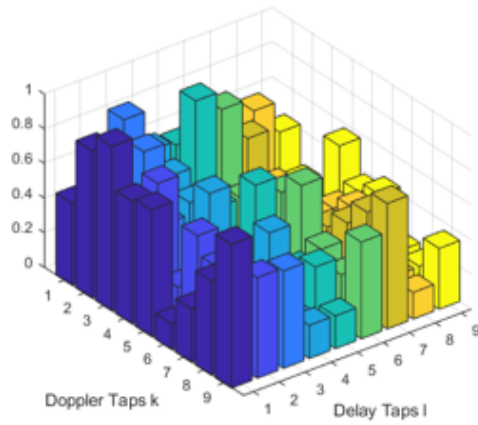
where  $j$  is the iteration number given by  $j = mM + n$ . At every  $j^{\text{th}}$  iteration  $N \times N$  portion of the image is selected, with the aim of minimizing the Mean Squared Error (MSE) given by :

$$MSE = E\{e_j^2\} = E\{(D(m, n) - y(m, n))_j^2\} \quad (30)$$

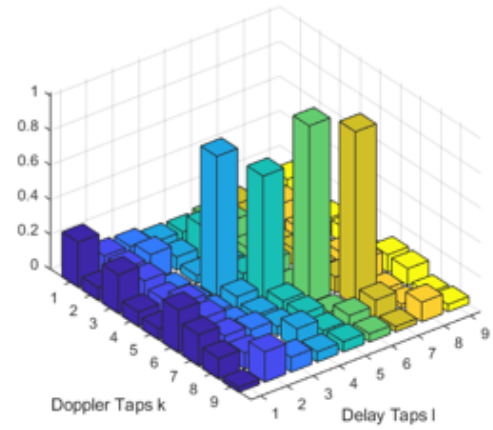
Here the filter window is smaller as compared to the image. But in the case of the OTFS system the channel coefficient matrix has a dimension of  $MN \times MN$  which is actually greater than the length of signal i.e.  $MN \times 1$ .

Thus instead of going for the TDLMS or any two dimensional adaptive algorithms, the one dimensional algorithms were combined with the pilot based approach. For the traditional pilot based methods, the pilot output in presence of noise will be dependent on the pilot power. Figure 7.6 (a) and (b) shows the pilot output at pilot power 2 dB and 10 dB respectively. The actual channel coefficients and estimated channel coefficients using pilot based approach and the combined approach are shown in Figure 7.7 at 10 dB pilot power. The combined approach gives the same results even at low pilot power.

In the time-frequency domain pilot addition approach, two methods were ex-



(a)



(b)

Figure 7.6: Pilot output grid at pilot power 2 dB (a) and 10 dB (b)

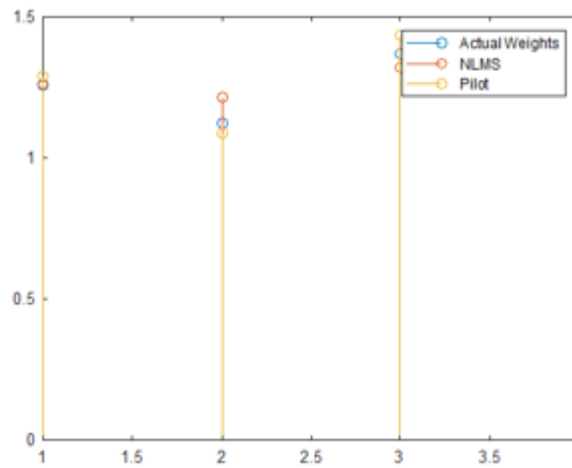


Figure 7.7: Estimated channel taps using adaptive algorithms

plained above. The simulation parameters for both the methods are given in Table 7.6 and Table 7.7 and the BER performance plots are shown in Figure 7.8 and Figure 7.10. The MSE curve is plotted in Figure 7.9 and Figure 7.11 for both these methods.

| Parameters                     | Value   |
|--------------------------------|---------|
| Num. of subcarriers (M)        | 16      |
| Num. f symbols (N)             | 12      |
| Length of pilot rows ( $N_p$ ) | 4       |
| Num. of pilot symbols( $N_S$ ) | 64      |
| Pilot power                    | 2 dB    |
| Carrier frequency( $f_c$ )     | 4 GHz   |
| Subcarrier spacing (f)         | 15 KHz  |
| SNR range                      | 0:20 dB |
| Modulation scheme              | QPSK    |

Table 7.6

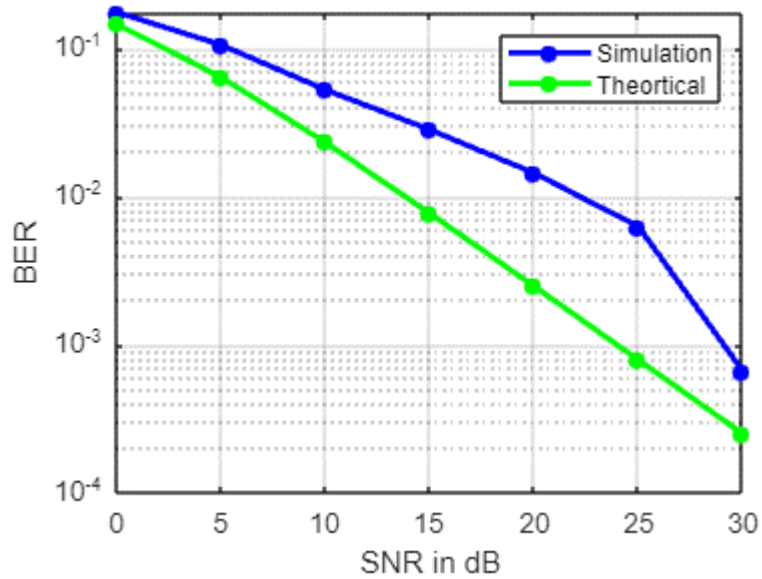


Figure 7.8: BER performance with block type pilot method

| Parameters                     | Value   |
|--------------------------------|---------|
| Num. of subcarriers (M)        | 16      |
| Num. f symbols (N)             | 16      |
| Num. of pilot symbols( $N_S$ ) | 16      |
| Pilot power                    | 2 dB    |
| Carrier frequency( $f_c$ )     | 4 GHz   |
| Subcarrier spacing (f)         | 15 KHz  |
| SNR range                      | 0:20 dB |
| Modulation scheme              | QPSK    |

Table 7.7

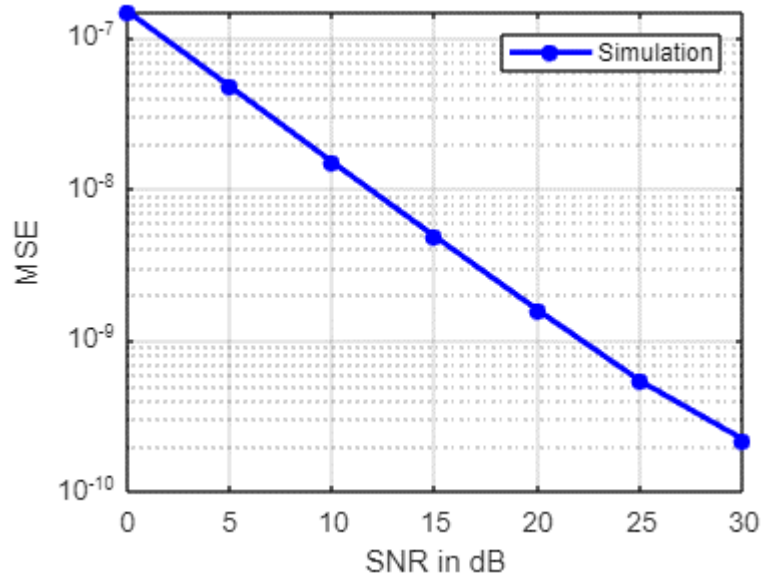


Figure 7.9: MSE performance with block type pilot method

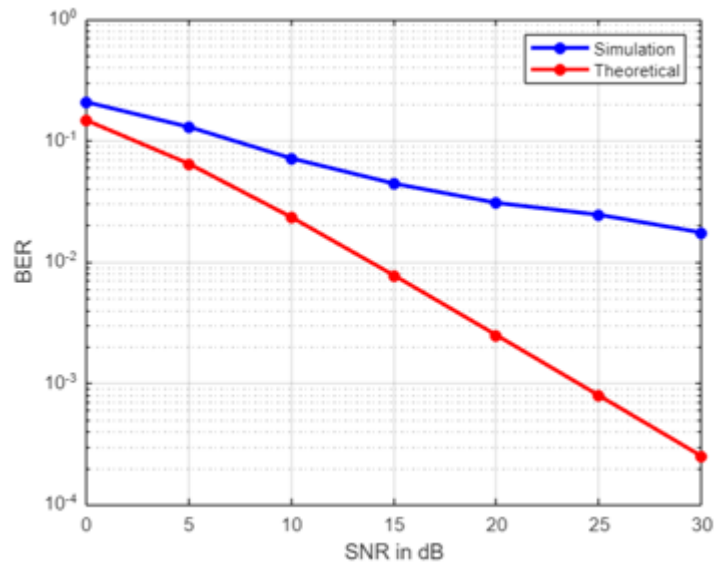


Figure 7.10: BER performance with comb and block type pilot symbols

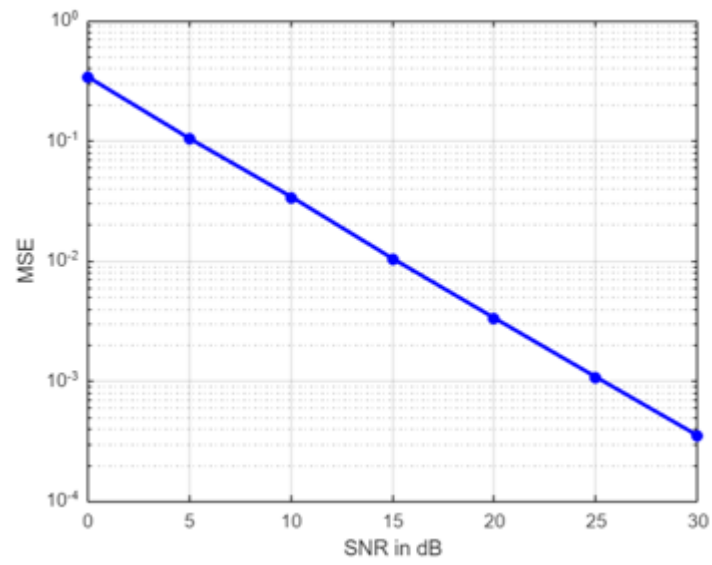


Figure 7.11: MSE performance with comb and block type pilot method



## CHAPTER 8

# Thesis Summary and Conclusion

In the introductory chapters, we have seen the need for the OTFS system. The problem addressed in this thesis was to estimate the channel for this OTFS system in an efficient and yet simple manner. The theory sections explained the key features of the OTFS system and the differences with respect to the conventional systems like OFDM system.

In the upcoming chapters, the existing channel estimation methods were introduced to solve the same problem. The performance of one of these methods i.e. the pilot based estimation method was evaluated in the simulation results section. The delay-Doppler domain estimation approached proposed in chapter 5, is when based on the pilot based method combined with adaptive algorithms. This method yields better results in noisy environment but with some additional requirement of time domain pilots.

Another approach proposed is based on time-frequency domain pilot insertion. There are two possible ways in which pilot symbols can be added to the grid as explained in Chapter 6. The number of pilot symbols used in both delay-Doppler based pilot method and the comb and block type time-frequency domain pilot based method is the same. The latter operates at a much lower pilot power but at the cost of some distortion caused due to the embedded pilots. So depending on the application any one of the algorithms can be used for channel estimation of the OTFS system.

## CHAPTER 9

### Future scope

In this thesis, the problem of channel estimation for the OTFS system was addressed from two perspectives. One was channel estimation in the delay-Doppler domain and other channel estimation in the time-frequency domain. The advantages and the limitations were also discussed in reference to the simulations and results provided for each method. Some of the issues related to the above mentioned methods can be addressed in future. For example, to investigate the time-frequency domain channel estimation approach ,if the discontinuity caused by the time-frequency domain pilot insertion can be minimized by designing some special filter.

In the delay-Doppler domain, some new adaptive algorithms can be explored for improvement. Also the ZAK transformation approach taken for the OTFS system model can be studied to explore other ways of estimating the channel.

## References

- [1] R. Hadani and A. Monk, "OtfS: A new generation of modulation addressing the challenges of 5g."
- [2] S. K. Mohammed, "Time-domain to delay-doppler domain conversion of ofts signals in very high mobility scenarios."
- [3] —, "Derivation of ofts modulation from first principles," vol. 70.
- [4] e. a. P. Raviteja, "Low-complexity iterative detection for orthogonal time frequency space modulation," *Proc. IEEE WCNC, Barcelona*.
- [5] —, "Interference cancellation and iterative detection for orthogonal time frequency space modulation," *Proc. IEEE WCNC, Barcelona*.
- [6] K. R. Murali and A. Chockalingam, "On ofts modulation for high doppler fading channels," *Proc. ITA*.
- [7] M. K. Ramachandran and A. Chockalingam, "Mimo-ofts in high doppler fading channels: Signal detection and channel estimation."
- [8] R. Hadani and A. M. Sayeed, "Delay-doppler channel estimation in almost linear complexity."
- [9] R. Hadani and S. Rakib, "Orthogonal time frequency space (otfs) modulation and applications."
- [10] W. Shen and R. W. Heath, "Channel estimation for orthogonal time frequency space (otfs) massive mimo," *IEEE Trans. Signal Process.*
- [11] A. Farhang and A. RezaZadeh, "Low complexity modem structure for ofdm-based orthogonal time frequency space modulation," *Proc. IEEE ICC*.
- [12] H. B. Mishra and P. Singh, "OtfS channel estimation and data detection designs with superimposed pilots."

- [13] S. Im, "A normalized block lms algorithm for frequency-domain volterra filters."
- [14] U. Hamid and A. M. Bhatti, "Application of adaptive filters in sensor array processing for underwater applications."
- [15] H.-C. Huang and J. Lee, "A new variable step-size nlms algorithm and its performance analysis."
- [16] S. Nunoo and U. A. K. Chude-Okonkwo, "Variable step-size l0-norm nlms algorithm for sparse channel estimation."
- [17] M. S. E. Abadi and S. Nikbakht, "Image denoising with two-dimensional adaptive filter algorithms."
- [18] M. M. HADHOUD and D. W. THOMAS, ""the two-dimensional adaptive lms [ tdlmsj algorithm."